AFRL-RX-WP-JA-2017-0333

FLEXIBLE GaN FOR HIGH PERFORMANCE, STRAINABLE RADIO FREQUENCY DEVICES (POSTPRINT)

Elizabeth A. Moore and Timothy Prusnick
Wyle Laboratories

Nicholas R. Glavin, Eric R. Heller, Benji Maruyama, and Donald L. Dorsey
AFRL/RX

Kelson D. Chabak, Dennis Walker, and Michael R. Snure
AFRL/RY

5 April 2017
Interim Report

AIR FORCE RESEARCH LABORATORY
MATERIALS AND MANUFACTURING DIRECTORATE
WRIGHT-PATTERSON AIR FORCE BASE, OH 45433-7750
AIR FORCE MATERIEL COMMAND
UNITED STATES AIR FORCE

REPORT DOCUMENTATION PAGE

Form Approved
OMB No. 0704-0188

1. REPORT DATE *(DD-MM-YY)*	2. REPORT TYPE	3. DATES COVERED *(From - To)*
5 April 2017	Interim	8 September 2014 – 5 March 2017

4. TITLE AND SUBTITLE
FLEXIBLE GaN FOR HIGH PERFORMANCE, STRAINABLE RADIO FREQUENCY DEVICES (POSTPRINT)

5a. CONTRACT NUMBER
FA8650-15-D-5405-0002

5b. GRANT NUMBER

5c. PROGRAM ELEMENT NUMBER
62102F

6. AUTHOR(S)
1) Elizabeth A. Moore and Timothy Prusnick - Wyle Laboratories
2) Nicholas R. Glavin, Eric R. Heller, Benji Maruyama, and Donald L. Dorsey - AFRL/RX
(continued on page 2)

5d. PROJECT NUMBER
4348

5e. TASK NUMBER 0002

5f. WORK UNIT NUMBER
X0YE

7. PERFORMING ORGANIZATION NAME(S) AND ADDRESS(ES)
1) Wyle Laboratories
2700 Indian Ripple Rd
Beavercreek, OH 45440
2) AFRL/RX
Wright-Patterson AFB
Dayton, OH 45433
(continued on page 2)

8. PERFORMING ORGANIZATION REPORT NUMBER

9. SPONSORING/MONITORING AGENCY NAME(S) AND ADDRESS(ES)
Air Force Research Laboratory
Materials and Manufacturing Directorate
Wright-Patterson Air Force Base, OH 45433-7750
Air Force Materiel Command
United States Air Force

10. SPONSORING/MONITORING AGENCY ACRONYM(S)
AFRL/RXAS

11. SPONSORING/MONITORING AGENCY REPORT NUMBER(S)
AFRL-RX-WP-JA-2017-0333

12. DISTRIBUTION/AVAILABILITY STATEMENT
Distribution Statement A. Approved for public release: distribution unlimited.

13. SUPPLEMENTARY NOTES
PA Case Number: 88ABW-2017-1573; Clearance Date: 5 Apr 2017. This document contains color. . Journal article published in Advanced Materials, Vol. 29, 20 Dec 2017. © 2017 Wiley-VCH. The U.S. Government is joint author of the work and has the right to use, modify, reproduce, release, perform, display, or disclose the work.
The final publication is available at https://doi.org/10.1002/adma.201701838

14. ABSTRACT ***(Maximum 200 words)***
Flexible and strainable Gallium Nitride (GaN) devices that transmit radio frequency (RF) signals efficiently over large distances will revolutionize the design of next generation wireless communication and infrastructure. We describe flexible GaN devices whose exceptional performance originates from the epitaxial growth on two-dimensional (2D) boron nitride which additionally allows for chemical-free transfer to a soft, flexible substrate. The GaN material heterostructures on a flexible substrate represent near state of the art values, with mobilities exceeding 2000 cm2/Vs and sheet carrier densities of 1.11 x 1013 cm-2, which are retained upon bending and straining up to 0.85% on 3D-printed conformal surfaces. In addition, the RF performance of flexible GaN high electron mobility transistor (HEMT) devices with an fT and fmax measured to be greater than 42 GHz and 74 GHz, respectively, up to 0.43% strain representing the first demonstrated flexible GaN HEMT for RF applications.

15. SUBJECT TERMS
Flexible RF electronics, Gallium Nitride, Flexible GaN

16. SECURITY CLASSIFICATION OF:			17. LIMITATION OF ABSTRACT:	18. NUMBER OF PAGES	19a. NAME OF RESPONSIBLE PERSON (Monitor)
a. REPORT	b. ABSTRACT	c. THIS PAGE			Lawrence Brott
Unclassified	Unclassified	Unclassified	SAR	10	19b. TELEPHONE NUMBER *(Include Area Code)* (937) 255-9157

REPORT DOCUMENTATION PAGE Cont'd

6. AUTHOR(S)

3) Kelson D. Chabak, Dennis Walker, and Michael R. Snure - AFRL/RY

7. PERFORMING ORGANIZATION NAME(S) AND ADDRESS(ES)

3) AFRL/RY, Wright-Patterson AFB, OH 45433

ADVANCED MATERIALS
www.advmat.de

Flexible Gallium Nitride for High-Performance, Strainable Radio-Frequency Devices

Nicholas R. Glavin, Kelson D. Chabak, Eric R. Heller, Elizabeth A. Moore, Timothy A. Prusnick, Benji Maruyama, Dennis E. Walker Jr., Donald L. Dorsey, Qing Paduano, and Michael Snure*

Flexible gallium nitride (GaN) thin films can enable future strainable and conformal devices for transmission of radio-frequency (RF) signals over large distances for more efficient wireless communication. For the first time, strainable high-frequency RF GaN devices are demonstrated, whose exceptional performance is enabled by epitaxial growth on 2D boron nitride for chemical-free transfer to a soft, flexible substrate. The AlGaN/GaN heterostructures transferred to flexible substrates are uniaxially strained up to 0.85% and reveal near state-of-the-art values for electrical performance, with electron mobility exceeding 2000 $cm^2 V^{-1} s^{-1}$ and sheet carrier density above $1.07 \times 10^{13} cm^{-2}$. The influence of strain on the RF performance of flexible GaN high-electron-mobility transistor (HEMT) devices is evaluated, demonstrating cutoff frequencies and maximum oscillation frequencies greater than 42 and 74 GHz, respectively, at up to 0.43% strain, representing a significant advancement toward conformal, highly integrated electronic materials for RF applications.

Future systems for use in wireless communication, the internet of things, autonomous vehicles, and radar applications will require small footprint, wide bandwidth, and high power devices of exceptional performance that are easily integrated into the world around us.[1–3] Over the last decade, gallium nitride (GaN) devices have been fundamental and essential elements to meet these requirements for high-power amplification of the radio frequency (RF) signal in MHz to GHz frequencies and beyond, especially for military applications.[4–6] As new demands for high-power conformal and flexible electronics for future fifth generation (5G) wireless communication operating as high as 100 GHz and speeds as high as 10 Gb s^{-1},[7] as depicted in **Figure 1**a, amplifiers based on GaN technology are prime candidates to replace existing Si or GaAs devices. The high cost of manufacturing has restricted the implementation of GaN-based amplifiers to mostly military applications, however, new demands for faster data speeds and smaller component sizes continue to drive next generation wireless systems where consumers will benefit significantly from the high power densities achievable in GaN devices.[8]

Further complicating the paradigm shift for 5G and new wireless capabilities, the reduction in signal propagation at higher frequencies will require an increase in the number of amplifiers needed for effective wireless infrastructure. To more effectively accomplish this, the entire wireless platform, including the RF devices, can be engineered to flex and conform toward integration on compact and mobile platforms. Allowing for the devices to accommodate strain is important in that it will ultimately reduce the 2D footprint of the device, enable wireless systems to be placed onto nonplanar platforms or surfaces, and improve overall mechanical reliability. The study herein describes a growth method to achieve flexible GaN films specifically for high performing RF devices. In addition, for the first time, RF characteristics of flexible T-gated GaN high electron mobility (HEMT) devices released from the substrate with the use of a 2D boron nitride (BN) mechanical release layer were demonstrated to be strainable and flexible. The flexible devices are shown in Figure 1b and transcend the conventional wisdom that flexibility in electronic systems leads to a significant drop in performance, as electron mobility exceeding 2000 $cm^2 V^{-1} s^{-1}$ at tensile strains as high as 0.85%, measured cutoff frequency, f_T, beyond 42 GHz and maximum oscillation frequencies, f_{max}, above 74 GHz at strain levels of 0.43% all reveal the potential for high-performance conformal, strainable wireless systems based on flexible GaN.

Since GaN grown by metal–organic chemical vapor deposition (MOCVD) requires growth temperatures greater than 1000 °C and stable crystalline substrates (Si, sapphire, SiC),[11,12] to ultimately achieve flexible devices, they must be transferred from the rigid growth substrate. Transfer of GaN films and devices has been performed using two main strategies; laser

Dr. N. R. Glavin, Dr. E. R. Heller, Dr. E. A. Moore, Dr. B. Maruyama, Dr. D. L. Dorsey
Air Force Research Laboratory
Materials and Manufacturing Directorate
Wright-Patterson AFB, OH 45433, USA
E-mail: Nicholas.Glavin.1@us.af.mil
Dr. K. D. Chabak, T. A. Prusnick, Dr. D. E. Walker Jr., Dr. Q. Paduano, Dr. M. Snure
Air Force Research Laboratory
Sensors Directorate
Wright-Patterson AFB, OH 45433, USA
Dr. E. A. Moore, T. A. Prusnick
KBRwyle
Dayton, OH 45431, USA

DOI: 10.1002/adma.201701838

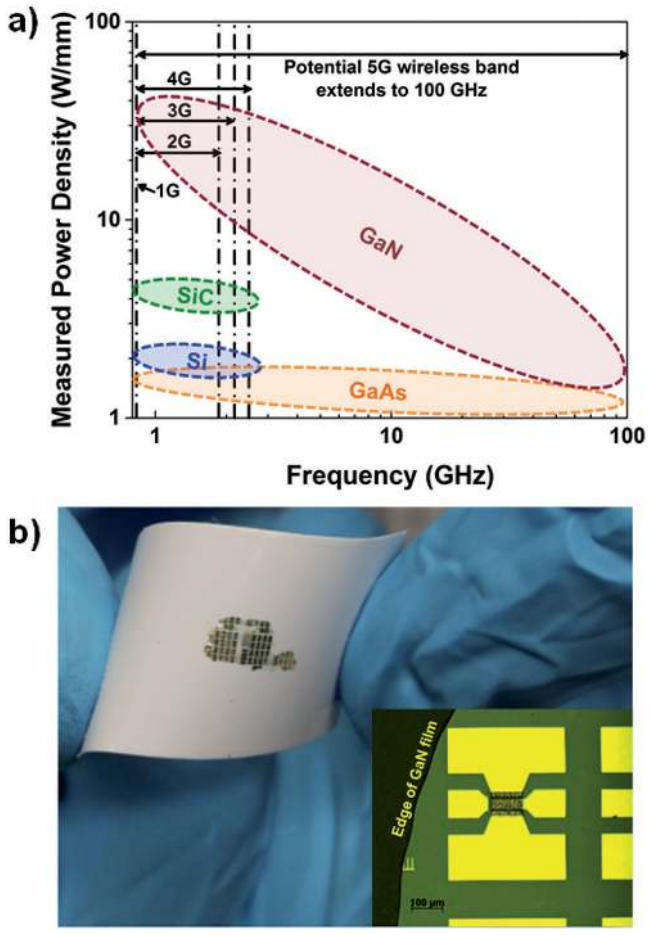

Figure 1. Measured power density of traditional RF amplifier materials at different frequencies and wireless generation bands, as well as an image of the flexible GaN devices. a) Measured RF power density at different operational frequencies for conventional RF amplifier materials[9,10] with the traditional wireless generation (first generation to fifth generation) frequency bands used within the United States, and b) image of ≈40 flexible GaN devices, with the inset showing a close-up of a flexible HEMT.

lift-off of the GaN film[13–15] or etching to chemically remove the substrate.[16–21] Growth of GaN on Si simplifies the substrate etching removal process and has hence been the most widely used approach for development of transferred GaN electronics. However, the GaN material grown on Si is typically of lower quality than when grown on sapphire or SiC due to the significant structural and lattice mismatch.[22] More recently, a method involving epitaxial lift-off processes through a sacrificial layer[23] or a 2D buffer layer,[24–27] such as graphene or *h*-BN, has demonstrated transfer of GaN devices for light-emitting diodes without the use of harsh chemicals or etchants. The initial demonstration of this technique has been successful in removal of GaN films, but has yet to demonstrate the transfer of high-quality GaN epitaxy to retain planar-processed, high-performance RF amplifier devices. In addition, RF performance of the transferred devices as a function of external strain, a critical evaluation for flexible RF devices, has yet to be reported. The development of flexible GaN films in this study as well as the evaluation of the RF performance of GaN HEMT devices under strain enables future flexible, high-performance RF systems that are necessary for the new paradigm shift in wireless communication systems.

Production of high-quality transferable GaN devices on van der Waals (vdW) layers has been facilitated by the recent availability of high-quality atomically smooth BN and graphene epitaxial layers. These layers serve multiple functions: providing a weak vdW interface for film lift-off and removal and acting as an epitaxial template for growth of GaN. The morphology and quality of the layer can be linked to GaN crystal quality and adhesion strength to the substrate. BN films with roughness greater than only a few angstroms resulted in poor GaN crystal quality and films which will spontaneously release from the substrate, highlighting the need for atomically smooth and flat BN.[28] Well ordered BN films are found to be the most ideal template for the combination of high-quality epitaxial growth, postgrowth device processing and mechanical lift-off. Using our recently developed process we produce wafer scale (2 in. diameter) few-layer BN films with excellent thickness uniformity (<5%) and low roughness (<0.1 nm RMS) that are ideally suited to produce flexible AlGaN/GaN HEMTs.[25] Flexible GaN HEMT structures consisting of a 15 nm AlN nucleation layer followed by a 1.5 μm thick Fe-doped GaN buffer, 0.5 μm undoped GaN layer, 2 nm AlN insert layer, 17 nm $Al_{0.27}Ga_{0.73}N$ boundary layer, and 3 nm GaN cap, were grown by MOCVD on a 1.6 nm BN layer on a sapphire substrate.[28] With the lack of dangling bonds on the sp^2-bonded BN surface, nucleation is the primary challenge to growth of a high-quality epitaxial layer. Various nucleation layers and functionalization methods have been reported to overcome the challenge of nucleation with variable success.[29–31] In this work, a thin pinhole free AlN nucleation layer was found to produce GaN and AlGaN/GaN structures with the lowest roughness and dislocation densities. If the AlN nucleation layer is greater than a few tens of nanometers strain between the nucleation and GaN layers can cause self-separation and buckling of the film. A cross-sectional transmission electron microscopy (TEM) image of this structure is shown in **Figure 2**a with high resolution images of the AlGaN/AlN/GaN and AlN/BN/sapphire interfaces shown in Figure 2b,c. Further characterization of the BN film growth on sapphire necessary for the heterostructure growth is highlighted in previous works.[28,32,33] High-resolution TEM images revealed the high-quality atomically abrupt interface between the GaN, AlN, and AlGaN layers. This quality is further illustrated by low surface roughness (<0.3 nm RMS) revealed by atomic force microscopy (AFM) (Figure 2d). X-ray rocking curves (Figure 2e) and two beam dark field TEM (Figure S1, Supporting Information) were used to quantify material quality with a measured threading dislocation density of $<3 \times 10^8$ cm^{-2}. The presented collection of characterization results demonstrates the ability to epitaxially grow GaN HEMT structures on a vdW surface with quality comparable to those on conventional substrates such as sapphire and SiC.[34,35]

Several GaN HEMT die were fabricated on a 2 in. sapphire wafer that included van der Pauw and transmission line measurement (TLM) test structures. To withstand device processing conditions, the AlGaN/GaN stack must remain flat and well adhered to the sapphire substrate to ensure good device yield and performance. The requirements of this step reiterate

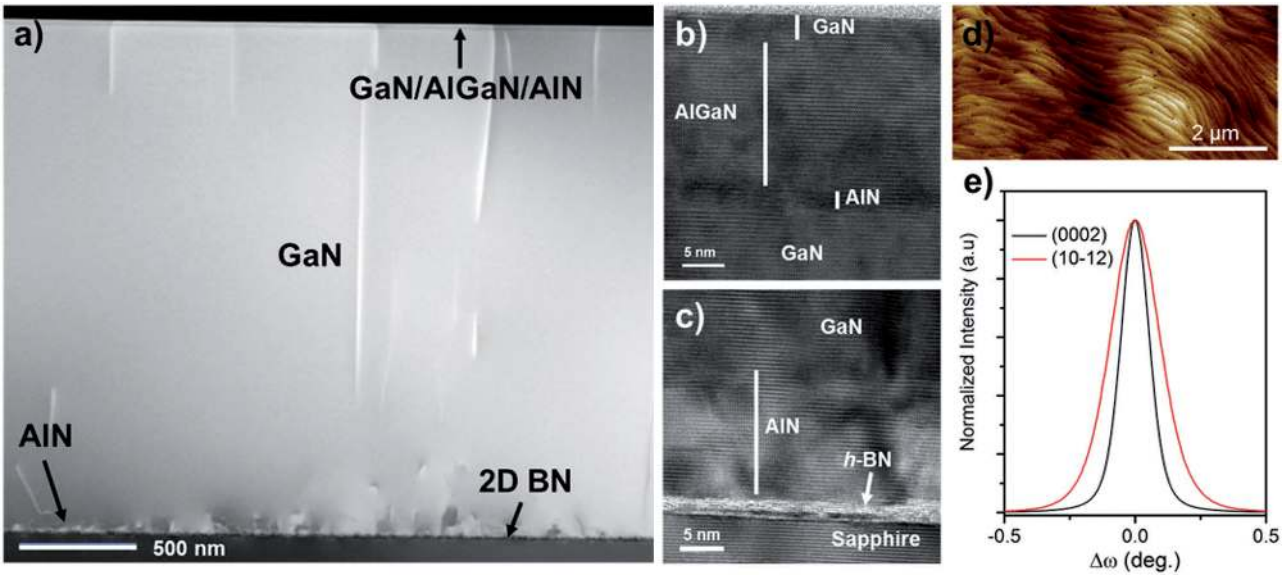

Figure 2. Analysis of the material heterostructure required for high-performance flexible GaN devices. a) Cross-sectional TEM image of GaN HEMT material stack, b) close-up TEM image of GaN/AlGaN/AlN interface, c) close-up TEM image of sapphire/*h*-BN/AlN/GaN interface, d) AFM image of the top surface, and e) X-ray rocking curve from the GaN on-axis (0002) and off-axis (10–12) with full-width half-maximum (FWHM) of 0.11° and 0.19°.

the need for a high-quality vdW buffer. After processing, the devices and test structures were able to be easily transferred to a 100 μm thick flexible 3M adhesive substrate by means of polydimethyl sulfoxide (PDMS) elastomeric stamping method (a more detailed process description is shown in Figure S5 in the Supporting Information).[36] The stamping method does not require any harsh chemicals or processing, and is favorable for cost reduction due to the fact that the growth substrate can be reused for future material depositions. During the transfer process, device structures remained completely intact and free from damage due to the gentle lift-off and transfer method.

To evaluate critical material properties of the flexible GaN under external applied strain, the GaN and 3M adhesive substrate were affixed to flat and under fixed bend radii of 48, 24, and 12 mm (image of bend radii test in **Figure 3**a). The estimated strain directly at the top of the structure can be calculated based upon the thickness of the material away from the neutral axis as a function of the bend radii applied using the $\Delta R/R$ method. The strain values at the 2DEG AlGaN/GaN interface, for a 48, 24, and 12 mm bend radii were calculated to be 0.21%, 0.43%, and 0.85% (with GaN and tape thickness totaling 102 μm and the top of the rigid backing assumed to be at the neutral axis).[37] In addition, the average strain in the AlGaN/GaN HEMT structure can be measured using Raman spectroscopy by evaluating the shift in the GaN E_2^H mode under the external applied strain. It is well established that tensile (compressive) strain in *c*-plane GaN results a blue (red) shift in this mode. Figure 3b shows the E_2^H mode measured from the same sample flat and flexed to a bend radii up to 12 mm. A blueshift of up to 0.3 cm^{-1} is evident when the transferred GaN film was taken from a flat state to the 12 mm radii. After bending and flattening, the GaN films revert back to the strain conditions before the experiment started. A total average shift of increasing tensile strain of 0.8% is measured in close agreement with the $\Delta R/R$ calculated values. The Raman studies described here reveal an important observation in that the strain applied to the flexible GaN films and devices are not simply accommodated by the underlying substrate, but are in fact imparting a reversible, temporary deformation of the GaN lattice from the external strain.

The post-transferred AlGaN/GaN material heterostructure on the flexible substrate exhibited extremely high measured mobility in a flat state at 2120 $cm^2\ V^{-1}\ s^{-1}$ and the value was reduced to 2005 $cm^2\ V^{-1}\ s^{-1}$ upon straining to the maximum bend radii of 12 mm (0.85% strain), as shown in Figure 3d using the van der Pauw structure shown in Figure 3c. The sheet carrier density appeared to exhibit the opposite trend with a change from 1.07 to 1.12×10^{-13} cm^{-2}, a total increase of 4.7%. At the maximum strain condition, an increase in n_s by 6.9×10^{11} cm^{-2} is expected due to increased piezoelectric induced charge,[38,39] which is very close to the measured value of 5.0×10^{11} cm^{-2} observed in the measurements here. The product of the mobility and sheet carrier density is directly related to the inverse of the sheet resistance, which slightly increases but remains within 1% of the starting value (as shown in Figure S6 in the Supporting Information). The values of mobility and sheet carrier density on the flexible tape far exceed previous reports of GaN HEMTs grown on 2D materials,[25] and represent state of the art electron transport behavior even for rigid AlGaN/GaN structures grown on conventional substrates.[40,41] The 2DEG transport properties reflect the excellent material quality and necessary importance for epitaxial growth of GaN on a high-quality 2D BN layer.[32] Similar GaN devices for lift-off and transfer are grown on silicon and are typically of lower quality due to a lattice mismatch of more than 17%, substrate bowing, and thermal expansion mismatch.[22] This leads to a reduction in 2DEG mobility of GaN devices on Si by as much as 10% as compared to the flexible devices measured here.

An optical image of a flexible 2×50 μm HEMT device with a gate length of 170 nm that was transferred from the growth substrate is shown in **Figure 4**a. The image of the undamaged

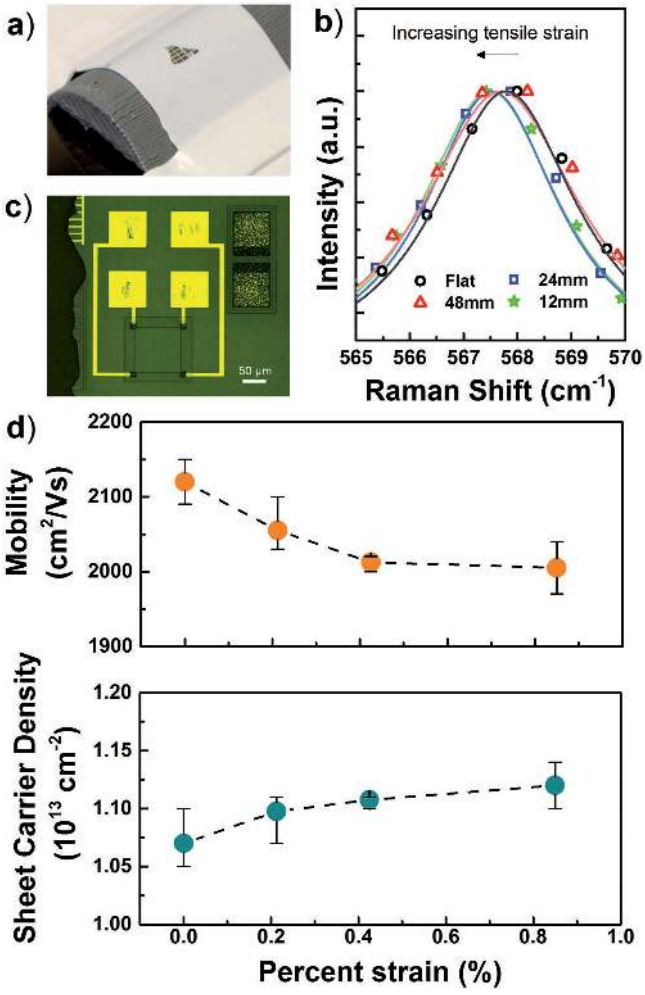

Figure 3. Influence of applied strain on the material properties of flexible GaN films. a) Image of GaN film with device structures conformed around a 3D printed 12 mm bend radii, b) Raman scan of E_2^H peak and the shift of peak position as a function of the applied strain, c) GaN van der Pauw test structure transferred to a flexible substrate for mobility and sheet-carrier-density measurements, and d) measured mobility and sheet carrier density of the flexible GaN films on tape substrate using strain values from the $\Delta R/R$ method. Error bars in (d) represent the maximum and minimum values retained upon four independent measurements.

device highlights the ability of the PDMS stamping method to transfer high-quality, fragile device structures without visible damage. Initial DC and RF characterization reveal that the electrical performance is retained upon transfer of the device to the flexible substrate. The change in substrate from the rigid, higher thermal conductivity sapphire to the flexible 3M adhesive tape resulted in a decrease in observed transconductance and drain current at forward gate bias voltage due to thermal effects (as depicted in Figure S7 in the Supporting Information). The reduction here at higher V_G is also observed in similar devices transferred to flexible substrates, where as much as a 90% reduction in RF power density as compared to GaN on SiC is observed.[18] For high-power applications flexible/conformal substrates such as metal foils could be used to overcome the self-heating limits imparted by the low thermal conductivity flexible substrates used here.

To evaluate the flexible electrical performance of the GaN devices, a transferred HEMT was conformed around the same 3D-printed cylinders as were used in the mobility measurements. The DC performance of the flexible GaN HEMTs appeared to be impacted by the applied strain, as portrayed in Figure 4b. In this case, the peak transconductance value ($G_{m,peak}$) and current density (I_D) at 0 V is reduced by a total of 8.1% and 7.7%, respectively, when comparing the device from the soft substrate in a flat state to a conformed state at 24 mm bend radii (0.43% estimated strain). After the device was moved to the 12 mm bend radii (0.83% estimated strain) the device failed during testing due to a crack forming through the device orthogonal to the strain direction presumably due to the increased piezoelectric strain as well as sample degradation,[42] and further testing could not be performed. The change in DC parameters as a function of strain is believed to be a combination of two independent mechanisms. The reduction in peak transconductance upon bending has been observed for other tests of similar GaN devices, and is presumed to be a product of the reduction in mobility as well as the inherent degradation and a change of strain state within the device.[43–45] The second indication of the physical impact on the DC performance is the shift in the threshold voltage (V_{TH}) of −0.03 and −0.17 V under the influence of 0.21% and 0.43% strain, respectively, which is related to the polarization-induced charge density increasing under applied tensile strain. Notably, the 2D electron gas (2DEG) at the AlGaN/GaN interface does not typically arise from ionized donors but instead from spontaneous and piezoelectric polarization difference between the Wurtzite GaN and AlGaN crystals.[38] The piezoelectric coefficient of AlGaN is greater than GaN, causing a net increase in the charge carrier density at the interface with tensile strain. The increase is estimated be 3.2×10^{11} cm^{-2} at the 0.43% strain condition for our structure, which is in excellent agreement to the measured 3.5×10^{11} cm^{-2} shown in Figure 3c. The resultant increase in carriers leads to a calculated shift in threshold voltage caused solely by the piezoexpansion effect that matches well with the observed data, and is shown in the inset of Figure 4b.[38]

Small signal RF gain characterization is shown in Figure 4c, where the cutoff frequency, f_T, and maximum oscillation frequency, f_{max}, at zero external applied strain was extrapolated with a −20 dB/dec fit to be 47 and 74 GHz, respectively, giving an RF figure of merit (the product of the cutoff frequency and gate length $f_T \times L_G$) equal to 8 GHz μm. This RF performance is superior to previously reported GaN HEMT studies limited to transfer onto a flat, soft substrate, which report an RF figure of merit <4.[18] Higher RF performance is presumably achieved as a result of the high-quality epitaxial layer transfer enabled by GaN growth on van der Waals 2D substrates rather than Si.[46] The extrapolated cutoff frequency is reduced by 9.0% under applied strain due to the linear relationship of cutoff frequency with DC transconductance. After 0.43% external applied strain, f_T slightly decreases to 42 GHz, as shown in Figure 4d. For the devices measured in this study, the f_{max} of the 0.17 μm gate length devices remains nearly constant (within 1% of the initial value) around 74 GHz throughout straining. This is a direct result of the unchanged device parasitics (R_C, R_{SH}) due to excellent material quality during growth, transfer, and straining, and a weaker dependence on transconductance as compared to f_T,

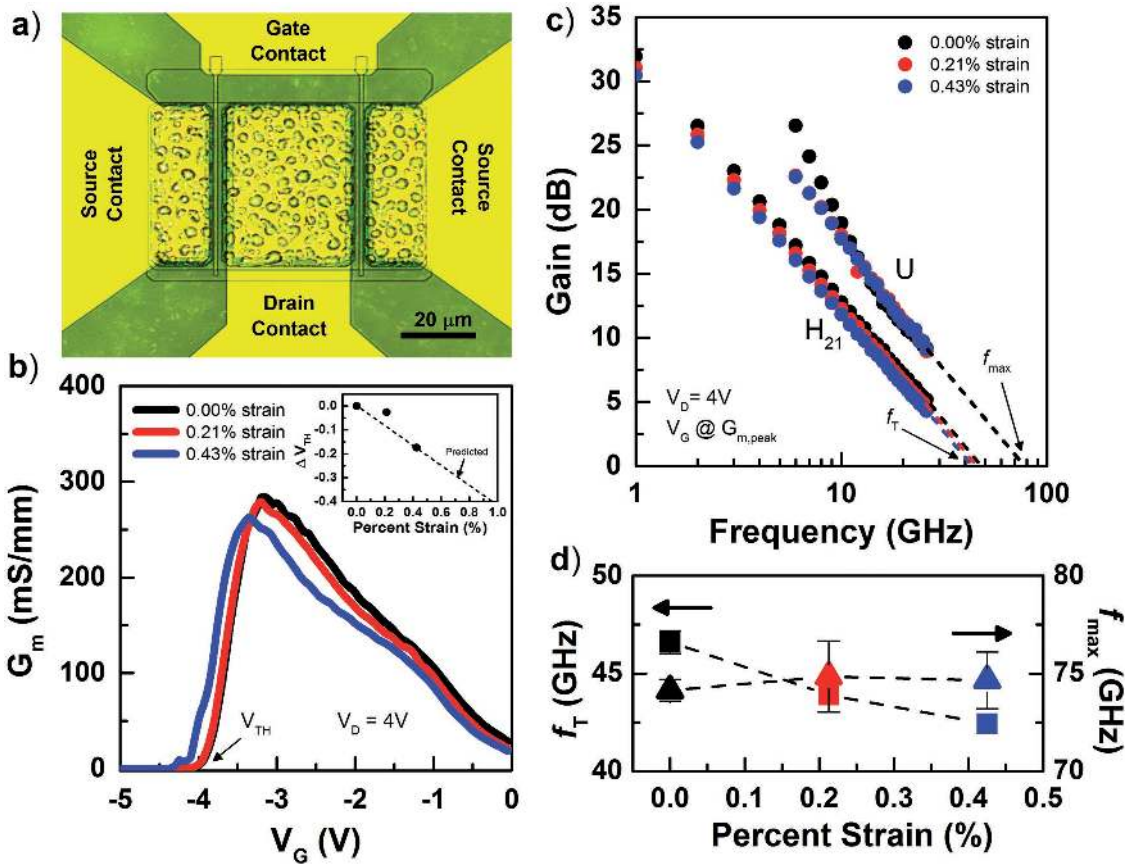

Figure 4. Device performance of flexible GaN HEMTs under applied external strain. a) Optical image of a transferred GaN HEMT device on a flexible substrate, b) plot portraying the change in DC parameters as the high-performance GaN devices are placed under an external strain as well as the predicted versus actual change in measured threshold voltage as a function of applied strain calculated by the $\Delta R/R$ method, and c) RF performance of the extrinsic current gain (H_{21}) and unilateral power gain (U) and linear extrapolation of f_T and f_{max}, and d) f_T (depicted as squares) and f_{max} (depicted as triangles) values for RF testing as a function of applied external strain.

where f_{max} is proportional to the square root of the transconductance.[47] The RF results reveal that the GaN material retains excellent f_{max} and a slight reduction in f_T at higher strain rates, but overall still behaves exceptionally well with regards to high-frequency performance. In future flexible and conformal RF systems, GaN devices strained beyond 0.43% tensile strain may require additional strain mitigation strategies during device operation.

It is clear that the growth of GaN on 2D BN is the key to unlocking high-quality flexible devices, as the BN serves two purposes; an epitaxial template for high-quality GaN that rivals state of the art for electrical performance, and providing for a means to transfer the devices without the use of harsh chemicals or etchants. The transferred flexible GaN/AlGaN structures are demonstrated to exhibit high electron mobility and sheet carrier density that exceeded 2000 $cm^2\ V^{-1}\ s^{-1}$ and $1.07 \times 10^{13}\ cm^{-2}$, respectively, and show inverse behavior upon straining. The GaN material is highly influenced by the applied strain in the observed piezoelectric-induced charge at the heterostructure interface. Flexible GaN HEMT devices display excellent DC and RF properties when exposed to as high as 0.43% strain with an extrapolated f_T and f_{max} at 42 and 74 GHz, respectively, corresponding to the first RF performance of a T-gated GaN HEMT transferred using a 2D release layer and under an external applied strain. The flexible, high performing GaN devices represent a major advancement for next generation strainable wireless communication that can result in a significant improvement in speed and bandwidth for both commercial and military systems.

Experimental Section

Boron nitride films were deposited by low pressure MOCVD on sapphire at 1000 °C from triethylboron and NH_3 with a V/III ratio of 2250 and pressure of 20 Torr. BN/sapphire templates were then loaded into an EMCORE D180 MOCVD system for growth of AlGaN/GaN (HEMT) structures. Ammonia, trimethylaluminum, trimethylgallium, and ferrocene were used as N, Al, Ga, and Fe precursors. A 15 nm thick AlN nucleation layer was deposited at 1000 °C using a V/III ratio of 2300 followed by a three step process for high temperature (1025 °C) growth of a 1.5 μm Fe doped GaN, 0.5 μm undoped GaN layer, 2 nm AlN insert layer, 17 nm AlGaN boundary layer with 27% Al, and 3 nm GaN cap layer.[29]

The AlGaN/GaN structures were characterized by high resolution TEM using a FEI Tecnai TF-20 FEG/TEM. Cross-sectional samples were prepared using the in situ FIB lift out technique on an FEI Dual Beam focused ion beam (FIB)/scanning electron microscope (SEM).

Surface morphology was measured by AFM using a Bruker Dimension Icon AFM operating in tapping mode. X-ray diffraction rocking curves of (0002) and $(10\bar{1}2)$, under symmetric and quasisymmetric ω-scan configurations respectively, using an Empyrean X'pert Pro system with a four bounce Ge monochrometer. Transport properties were measured at room temperature using an Accent 5500 Hall-effect measurement system and Leighton LEI contactless system.

AlGaN/GaN HEMTs were fully fabricated on the 2D BN/Sapphire substrate. First, electrical mesa isolation was achieved by inductively coupled plasma with $BCl_3/Cl_2/Ar$ chemistry to a depth of ≈80 nm. Ohmic contacts consisting of Ti/Al/Ni/Au were deposited by electron beam evaporation and subjected to rapid thermal annealing at 850 °C for 30 s in nitrogen ambient. Next, electron beam lithography T-gates with nominal 0.17 µm gate length were formed with trilayer poly(methyl methacrylate) (PMMA)/methyl methacrylate (MMA)/PMMA resist process and metallized with Ni/Au to form a Schottky gate contact. Metal interconnects with RF pad layout were patterned and metallized with Ti/Au, and a 200 nm Si_3N_4 passivation layer was finally deposited and etched with CF_4/O_2 reactive ion etching.

Process control monitor and TLM structures were used for four-point probe DC measurements on a Keithley 450 test system. The DC and RF performance of the HEMTs were characterized with an automated system consisting of an HP4142 parametric analyzer and HP8510 network analyzer with Cascade probes. S-parameters were measured from 1 to 26 GHz at $V_{DS} = 4$ V and V_{GS} equal to the gate bias corresponding to peak transconductance.

Supporting Information

Supporting Information is available from the Wiley Online Library or from the author.

Acknowledgements

The material is based upon work supported by the Air Force Office of Scientific Research under Award No. FA9550-16RYCOR331. TEM was performed by the Evans Analytical Group.

Conflict of Interest

The authors declare no conflict of interest.

Keywords

flexible GaN, flexible RF electronics, gallium nitride

Received: April 3, 2017
Revised: July 28, 2017
Published online: November 2, 2017

[1] A. Vinel, W. S. E. Chen, N. N. Xiong, S. Rho, N. Chilamkurti, A. V. Vasilakos, *IEEE Wirel. Commun.* **2016**, *23*, 8.
[2] N. Petrone, I. Meric, T. Chari, K. L. Shepard, J. Hone, *IEEE J. Electron Devices Soc.* **2015**, *3*, 44.
[3] Y. H. Jung, H. Zhang, S. J. Cho, Z. Ma, *IEEE Trans. Electron Devices* **2017**, *64*, 5.
[4] R. S. Pengelly, S. M. Wood, J. W. Milligan, S. T. Sheppard, W. L. Pribble, *IEEE Trans. Microwave Theory Techn.* **2012**, *60*, 1764.
[5] M. Asif Khan, A. Bhattarai, J. N. Kuznia, D. T. Olson, *Appl. Phys. Lett.* **1993**, *63*, 1214.
[6] M. Asif Khan, J. N. Kuznia, D. T. Olson, W. J. Schaff, J. W. Burm, M. S. Shur, *Appl. Phys. Lett.* **1994**, *65*, 1121.
[7] 4G Americas, *5G Technology Evolution Recommendations* (accessed: October 2015).
[8] C. S. Whelan, N. J. Kolias, S. Brierley, C. MacDonald, S. Bernstein, in *CS MANTECH Conf.*, Boston, MA, USA April **2012**).
[9] R. C. Fitch, D. E. Walker, A. J. Green, S. E. Tetlak, J. K. Gillespie, R. D. Gilbert, K. A. Sutherlin, W. D. Gouty, J. P. Theimer, G. D. Via, K. D. Chabak, G. H. Jessen, *IEEE Electron Device Lett.* **2015**, *36*, 1004.
[10] N. D. Du Toit, R. Thomas, J. H. Smith, F. N. Schirk, J. A. Mogel, *Microwave J.* **2010**, *53*, 90.
[11] W.-C. Huang, C.-M. Chu, Y.-Y. Wong, K.-W. Chen, Y.-K. Lin, C.-H. Wu, W.-I. Lee, E.-Y. Chang, *Mater. Sci. Semicond. Process.* **2016**, *45*, 1.
[12] X. L. Wang, C. M. Wang, G. X. Hu, J. X. Wang, T. S. Chen, G. Jiao, J. P. Li, Y. P. Zeng, J. M. Li, *Solid-State Electron.* **2005**, *49*, 1387.
[13] U. Tetsuzo, I. Masahiro, Y. Masaaki, *Jpn. J. Appl. Phys.* **2011**, *50*, 041001.
[14] J. Xu, R. Zhang, Y. P. Wang, X. Q. Xiu, B. Shen, S. L. Gu, Y. Shi, Z. G. Liu, Y. D. Zheng, *Mater. Lett.* **2002**, *56*, 43.
[15] W. S. Wong, T. Sands, N. W. Cheung, *Appl. Phys. Lett.* **1998**, *72*, 599.
[16] M. Schauler, F. Eberhard, C. Kirchner, V. Schwegler, A. Pelzmann, M. Kamp, K. J. Ebeling, F. Bertram, T. Riemann, J. Christen, P. Prystawko, M. Leszczynski, I. Grzegory, S. Porowski, *Appl. Phys. Lett.* **1999**, *74*, 1123.
[17] N. P. Pham, M. Rosmeulen, Z. Li, D. Sabuncuoglu, H. Osman, presented at 2013 IEEE 15th Electronics Packaging Technology Conf. (EPTC 2013), Singapore, December **2013**.
[18] S. Mhedhbi, M. Lesecq, P. Altuntas, N. Defrance, E. Okada, Y. Cordier, B. Damilano, G. Tabares-Jiménez, A. Ebongué, V. Hoel, *IEEE Electron Device Lett.* **2016**, *37*, 553.
[19] J. H. Choi, J. Kim, H. Yoo, J. Liu, S. Kim, C.-W. Baik, C.-R. Cho, J. G. Kang, M. Kim, P. V. Braun, S. Hwang, T.-S. Jung, *Adv. Opt. Mater.* **2016**, *4*, 505.
[20] M. Lesecq, V. Hoel, A. L. d. Etangs-Levallois, E. Pichonat, Y. Douvry, J. C. D. Jaeger, *IEEE Electron Device Lett.* **2011**, *32*, 143.
[21] S. Mhedhbi, M. Lesecq, P. Altuntas, N. Defrance, Y. Cordier, B. Damilano, G. Tabares Jimenéz, A. Ebongue, V. Hoel, *Phys. Status Solidi A* **2017**, *214*, 1600484.
[22] H. P. Lee, J. Perozek, L. D. Rosario, C. Bayram, *Sci. Rep.* **2016**, *6*, 37588.
[23] D. J. Meyer, B. P. Downey, D. S. Katzer, N. Nepal, V. D. Wheeler, M. T. Hardy, T. J. Anderson, D. F. Storm, *IEEE Trans. Semiconduct. Manuf.* **2016**, *29*, 384.
[24] Y. Kobayashi, K. Kumakura, T. Akasaka, T. Makimoto, *Nature* **2012**, *484*, 223.
[25] M. Hiroki, K. Kumakura, Y. Kobayashi, T. Akasaka, H. Yamamoto, T. Makimoto, presented at 2014 4th IEEE Int. Workshop on Low Temperature Bonding for 3D Integration (LTB-3D), Tokyo, Japan, July **2014**.
[26] T. Ayari, S. Sundaram, X. Li, Y. E. Gmili, P. L. Voss, J. P. Salvestrini, A. Ougazzaden, *Appl. Phys. Lett.* **2016**, *108*, 171106.
[27] J. Kim, C. Bayram, H. Park, C.-W. Cheng, C. Dimitrakopoulos, J. A. Ott, K. B. Reuter, S. W. Bedell, D. K. Sadana, *Nat. Commun.* **2014**, *5*, 4836.
[28] M. Snure, G. Siegel, D. C. Look, Q. Paduano, *J. Cryst. Growth* **2017**, *464*, 168.
[29] S. P. Qing, S. Michael, B. James, W. C. Z. Timothy, *Appl. Phys. Express* **2014**, *7*, 071004.
[30] N. Neeraj, D. W. Virginia, J. A. Travis, J. K. Francis, A. M. Michael, L. M.-W. Rachael, B. Q. Syed, A. F. Jaime, C. H. Sandra, O. N. Luke, G. W. Scott, G. Kurt, Charles R Eddy Jr., *Appl. Phys. Express* **2013**, *6*, 061003.

[31] H. Yoo, K. Chung, Y. S. Choi, C. S. Kang, K. H. Oh, M. Kim, G.-C. Yi, *Adv. Mater.* **2012**, *24*, 515.
[32] Q. Paduano, M. Snure, G. Siegel, D. Thomson, D. Look, *J. Mater. Res.* **2016**, *31*, 2204.
[33] Q. Paduano, M. Snure, D. Weyburne, A. Kiefer, G. Siegel, J. Hu, *J. Cryst. Growth* **2016**, *449*, 148.
[34] Z. Y. Xu, F. J. Xu, J. M. Wang, L. Lu, Z. J. Yang, X. Q. Wang, B. Shen, *J. Cryst. Growth* **2016**, *450*, 160.
[35] Z. J. Reitmeier, S. Einfeldt, R. F. Davis, X. Zhang, X. Fang, S. Mahajan, *Acta Mater.* **2010**, *58*, 2165.
[36] M. A. Meitl, Z.-T. Zhu, V. Kumar, K. J. Lee, X. Feng, Y. Y. Huang, I. Adesida, R. G. Nuzzo, J. A. Rogers, *Nat. Mater.* **2006**, *5*, 33.
[37] K. J. Lee, J. Lee, H. Hwang, Z. J. Reitmeier, R. F. Davis, J. A. Rogers, R. G. Nuzzo, *Small* **2005**, *1*, 1164.
[38] O. Ambacher, J. Majewski, C. Miskys, A. Link, M. Hermann, M. Eickhoff, M. Stutzmann, F. Bernardini, V. Fiorentini, V. Tilak, B. Schaff, L. F. Eastman, *J. Phys.: Condens. Mater.* **2002**, *14*, 3399.
[39] S. Shervin, S.-H. Kim, M. Asadirad, S. Ravipati, K.-H. Lee, K. Bulashevich, J.-H. Ryou, *Appl. Phys. Lett.* **2015**, *107*, 193504.
[40] H. C. Silvia, K. Stacia, T. Maher, L. Haoran, R. Brian, P. D. Steven, K. M. Umesh, *Semicond. Sci. Technol.* **2016**, *31*, 065008.
[41] J. Zhang, Y. Hao, J. Zhang, J. Ni, *Sci. China Ser. F: Inf. Sci.* **2008**, *51*, 780.
[42] E. Zanoni, M. Meneghini, G. Meneghesso, D. Bisi, I. Rossetto, A. Stocco, presented at 2015 IEEE 3rd Workshop on Wide Bandgap Power Devices and Applications (WiPDA), Blacksburg, Virginia, USA, November **2015**.
[43] K. J. Lee, M. A. Meitl, J.-H. Ahn, J. A. Rogers, R. G. Nuzzo, V. Kumar, I. Adesida, *J. Appl. Phys.* **2006**, *100*, 124507.
[44] M. Tapajna, R. J. T. Simms, Y. Pei, U. K. Mishra, M. Kuball, *IEEE Electron Device Lett.* **2010**, *31*, 662.
[45] S. Mukherjee, Y. Puzyrev, J. Chen, D. M. Fleetwood, R. D. Schrimpf, S. T. Pantelides, *IEEE Trans. Electron Devices* **2016**, *63*, 1486.
[46] W. Yuh-Renn, M. Singh, J. Singh, *IEEE Trans. Electron Devices* **2006**, *53*, 588.
[47] K. D. Chabak, X. Miao, C. Zhang, D. E. Walker, P. K. Mohseni, X. Li, *IEEE Electron Device Lett.* **2015**, *36*, 445.

